Thin Film Water on Muscovite Mica

Will Cantrell and George E. Ewing*

Department of Chemistry, Indiana University, Bloomington, Indiana 47405

Received: November 28, 2000; In Final Form: April 2, 2001

We have shown that water adsorbed to the (001) plane of muscovite mica has an infrared spectrum consistent with a bonding network that is more structured than that found in bulk water. Isotherms taken at temperatures ranging from near the ice melting point to room temperature suggest that water wets mica incompletely. Additionally, we find that the enthalpy and entropy of the adsorbed water molecules imply a strongly bound first layer. Both enthalpy and entropy approach the bulk values as the thickness of the adsorbed layer increases.

1. Introduction

An interface is commonly defined as a plane demarcating the boundary between two regions of adjoining space.[1] This mathematical definition implies that the interface is discontinuous. However, a physical interface separating phases cannot be discontinuous since the atoms, molecules or ions that define it are described by wave functions which are (in principle) infinite in extent. Moreover, the properties of one phase influence those of an adjacent phase, blurring the interface. The transition from one to another becomes not a step-function, but a profile, whose descriptions go back to the work of Gibbs[2] and Drude.[3] The shape of that profile reflects the type and strengths of the interactions between one phase and another and has myriad practical consequences ranging from adhesion and lubrication[4] to cloud formation.[5]

Muscovite mica is a popular choice for the study of interfacial phenomena because its almost perfect cleavage along the (001) plane removes the complexities introduced by surface roughness. Furthermore, water has an affinity for the surface of mica. Yet despite its study since at least 1918,[6] the adsorption of water to mica remains the subject of some ambiguity.

Following Turnbull and Vonnegut's conjecture that a close match between lattice constants of ice and a substrate might facilitate the liquid water-ice phase transition,[7] Jaffray et al.[8] and Bryant et al.[9] investigated mica as a possible candidate as an effective ice nucleating agent. Water molecules adhering to mica should already be in a configuration close to the crystalline structure of ice, reducing the degree of supercooling necessary to induce nucleation. However, mica did not initiate nucleation until the water was supercooled to −10 °C. These results seem to contradict the studies of Elbaum and Lipson,[10] who studied the dynamic behavior of "thick" (∼110 nm) films of liquid water as they dried. All of their measurements were made with "deeply supercooled water," some at temperatures approaching −30 °C. These observations beg the question as to why such deep supercooling is needed to induce the phase transition if the substrate lattice is close to that of ice.

More recently, explicit studies of the water−mica interface have suggested the presence of an ice-like water layer, even at room temperature.[11,12] Scanning polarization force microscopy (SPFM) studies showed the formation of metastable, polygon shaped islands, which had an epitaxial relationship with the underlying substrate. These islands were hypothesized to be ice-like in nature. Subsequent experiments with sum-frequency generation (SFG) vibrational spectroscopy showed that D_2O on mica adopted a predominately ordered structure. The same experiment showed no free OD bonds at the interface of the vapor and adsorbed D_2O layer. Molecular dynamics simulations of water on the (001) plane of mica also indicate that the first layer should form a stable, ice-like configuration with no free OH bonds at the interface separating the adsorbed layer and the vapor.[13]

The thickness of the adsorbed layer as a function of relative humidity is also an issue of some ambiguity. Using ellipsometry, Beaglehole et al.[14] determined that water wet mica incompletely, arriving at a film thickness of between one and two nanometers at saturation. They inferred a coverage of one statistical monolayer at 75% relative humidity. In contrast, Miranda et al.[12] concluded that a monolayer was formed only as the relative humidity approached 90%. Though it clouds the picture even further, it should be noted that Elbaum and Lipson[10] report that water wets mica completely.

Our approach to understanding the structure and properties of thin film water on mica is through a study by Fourier transform infrared (FTIR) spectroscopy. In the following, we describe absorbance measurements and adsorption isotherms over a range of temperatures. These isotherms yield thermodynamic values for the adsorption process. From spectroscopic band shapes, the hydrogen bond networks that stabilize thin film water are inferred.

2. Experiment

The sample cell for the thin film water studies, shown in Figure 1, was capped by silicon windows. It was thermostated with a recirculating bath from a variable temperature unit (Julabo FP50). The temperature, accurate to ±0.2 °C, was monitored with a type K thermocouple and Omega temperature readout DP460. The cell was evacuated with a diffusion pump (Varian HS-2), backed by a roughing pump (Welch DuoSeal). The mica (Ward Scientific), which was collected in the vicinity of Madras, India, was cleaved in room air, and placed within 5 min into the sample cell. The individual sheets of mica (eight for the experiments described here) were separated by 0.1 mm diameter Ta wire so that a total of 16 mica surfaces were exposed to the vapor. Spectrophotometric grade water (Alfa Aesar), which had been further purified by repeated freeze−pump−thaw cycles,

* To whom correspondence should be sent. E-mail: ewingg@indiana.edu

10.1021/jp004305b CCC: $20.00
Published on Web 05/17/2001

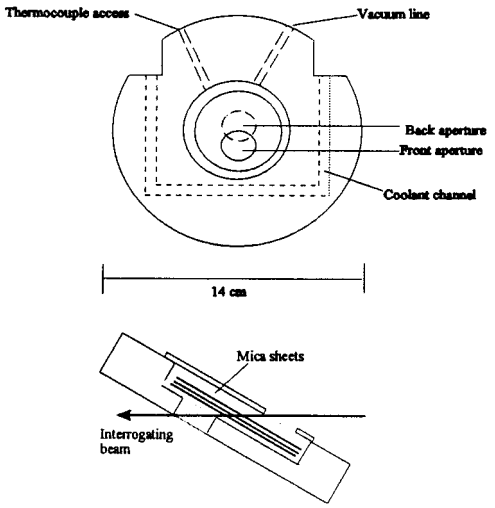

Figure 1. Upper panel is a schematic of the cell. The body of the cell is aluminum. The silicon windows (not shown) are offset to allow the IR beam to traverse the chamber when it is canted at the Brewster angle, shown in the lower panel.

was used as the reservoir for water vapor. The vapor pressure, in the range of 1 to 30 mbar, was monitored, with an accuracy of 10%, by Baratron gauges (MKS Instruments, Inc.).

The cell was placed into the spectrometer compartment, which was then purged with dry nitrogen to minimize interference from water vapor. To reduce the effects of Etalon fringing, the sample cell was canted at 57°, the nominal Brewster angle for mica. The interrogating beam was polarized in the plane of incidence (TM or E_p polarization) with a BaF_2 wire grid polarizer (International Crystal Laboratories).

Vibrational spectra with a resolution of 4 cm^{-1} were recorded with a Bruker IFS-66 FTIR spectrometer equipped with a liquid nitrogen-cooled InSb (indium antimonide) detector. The background and sample interferograms were transformed with a Blackman−Harris three point apodization function and 2× zero filling. The integrated absorbance of water films were obtained by numerical integration. Interfering water vapor absorption features were reduced with the use of a suitably scaled spectrum of the sample cell with only water vapor present.

3. Results and Discussion

3.1 Spectroscopy. A spectrum of a single sheet of mica of approximately 65 μm thickness, positioned orthogonal to unpolarized radiation, is shown on the upper panel of Figure 2. The light loss, because it is a consequence of both absorption and reflection, is expressed as extinction, $E = \log_{10} I_0/I$ where I_0 is the intensity through the cell before the mica was inserted and I after the sheet was in place. The light loss centered near 3600 cm^{-1} is associated with absorption by −OH stretching modes within the mica. The extinction value of $E > 3$ corresponds to less than 0.1% of light penetrating the mica—the mica is essentially opaque in this region. The Etalon fringes, illustrated on a finer scale in the inset to the upper panel of Figure 2, are due to interference caused by reflection of the beam within the mica. The magnitude of these features, $E \approx 0.01$, is greater than the absorbance due to thin film water by orders of magnitude, as we shall see, and clearly must be reduced.

The reflections which cause these annoying fringes can be effectively eliminated by canting the mica (by canting the cell) at its Brewster angle of 57°. This is demonstrated in the lower panel of Figure 2 for the cell containing 8 sheets of mica. The

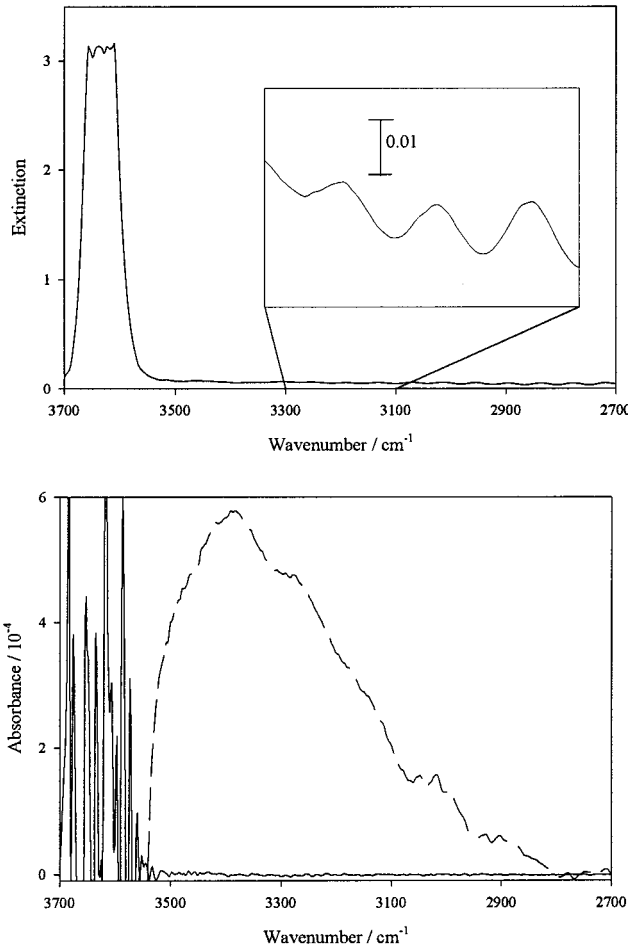

Figure 2. Extinction spectrum of muscovite mica (upper panel) illustrating the strong absorption feature centered near 3600 cm^{-1} and etalon fringes (inset to the upper panel). Zero absorbance (solid curve, lower panel) illustrates the noise level. Absorbance spectrum of water absorbed to mica (dashed curve, lower panel), illustrating the characteristic feature of thin film water.

solid line is a presentation of $A = \log_{10} (I'/I'')$ where I' is the intensity through the evacuated cell for one series of FTIR scans and I'' is the intensity through the cell with a second series of scans. We identify this as the zero absorbance line because, in principle, there should be no signal. The resulting zero absorbance in the region 2700−3500 cm^{-1} with peak-to-peak values of $\pm 5 \times 10^{-6}$, effectively the noise level, provides a useful lower limit for thin film absorbance measurements. The chaotic absorbance swings from 3550 to 3700 cm^{-1} are the consequences of photometric response breakdown due to the opacity of mica in this region. The solid line in the lower panel of Figure 2 thus shows a clear window from 2700 to 3500 cm^{-1} for the photometric study of thin film water.

The dashed curve in Figure 2 is the absorbance of thin film water on the mica sheets for a vapor pressure of 20 mbar at a temperature of 21 °C. Here, we have constructed $A = \log_{10} (I_0/I)$ where I_0 is the intensity through the cell with mica sheets only and I the intensity with water vapor added. The diffuse absorption spanning several hundred wavenumbers is centered at 3400 cm^{-1}. We shall discuss the significance of this spectroscopic profile in some detail later. For now, we shall use the photometric data to extract coverage information.

3.2 Isotherms. Canting the mica at the Brewster angle to effectively eliminate Etalon fringes reduces what were extinction spectra to absorbance spectra. We use a modified form of Beer's

law, discussed elsewhere,[15] to estimate the extent of the water coverage on the mica.

The absorbance is given by

$$A = \log_{10}\left(\frac{I_0}{I}\right) = \frac{N\sigma\,\rho\,t}{2.303\cos\phi_B} \tag{1}$$

where A is the absorbance as a function of wavenumber, I_0 and I are the transmitted intensities for the bare mica and mica with water adsorbed. respectively. N is the number of mica surfaces exposed to the vapor, σ is the wavenumber dependent cross section of liquid water, ρ is the density of water, t is the thickness of the adsorbed layer, and ϕ_B is the Brewster angle. The factor of 2.303 in the denominator is $\log_{10}(e)$.

To capture information across the absorption profile, we integrate eq 1 from 2700 to 3500 cm^{-1}. The only thing on the right-hand side of eq 1 which depends on wavenumber, $\tilde{\nu}$, is the cross section, σ. The integrated cross section is given by

$$\bar{\sigma} = \left(\frac{4\pi}{\rho}\right)\int_{\text{band}} \kappa\tilde{\nu}\,d\tilde{\nu} \tag{2}$$

where κ is the extinction coefficient for liquid water.[16]

We can replace ρt by S_{H_2O}, the density of water molecules on the surface and write the integrated absorbance as

$$\bar{A} = \frac{N\bar{\sigma}\,S_{H_2O}}{2.303\cos\phi_B} \tag{3}$$

Equation 3 can be solved for S_{H_2O}, and the water adlayer coverage defined as

$$\theta = \frac{S_{H_2O}}{S_{\text{mica}}} \tag{4}$$

where $S_{\text{mica}} = 1.2 \times 10^{15}$ cm^{-2} is the density of adsorption sites on the mica surface taken to be the O^- ions.[17]

Uncertainty in our derived coverages arises principally from the integrated absorbance and the assumed values of the integrated cross section of water. These uncertainties vary as a function of coverage. The spectra at low coverages are noisier than those at high coverages and thus affect the values of the integrated absorbances. The cross section (either at a specified wavenumber or integrated) also changes as a function of coverage because it is sensitive to the nature of the hydrogen bonding network.[18] For instance, the liquid to ice phase transition in water almost doubles the integrated cross section and shifts the position of the maximum cross section by 200 cm^{-1}.[19] In the water−mica system, the cross section will change from some initial value representative of water bonded to mica at submonolayer coverages to an intermediate value for one or so layers where the water is affected by both substrate and other water molecules. At the highest coverages, the cross section should be close to that of the bulk value.

Five isotherms for temperatures between 0.6 and 25.1 °C are shown in Figure 3. Using eqs 1−4, we calculated the coverage, θ. It is plotted against the reduced pressure, p/p_s, which is the ratio of the pressure of the vapor over mica, p, to its equilibrium value over liquid water at the specified temperature, p_s.

The shape of each of the isotherms is qualitatively the same. There is a near linear increase in coverage with p/p_s in the submonolayer regime followed by an steeper rise in coverage beyond $p/p_s \approx 0.8$. That the isotherms on increasing or decreasing pressures track each other indicates no evidence of hysteresis. However, there *are* subtle differences in the isotherms

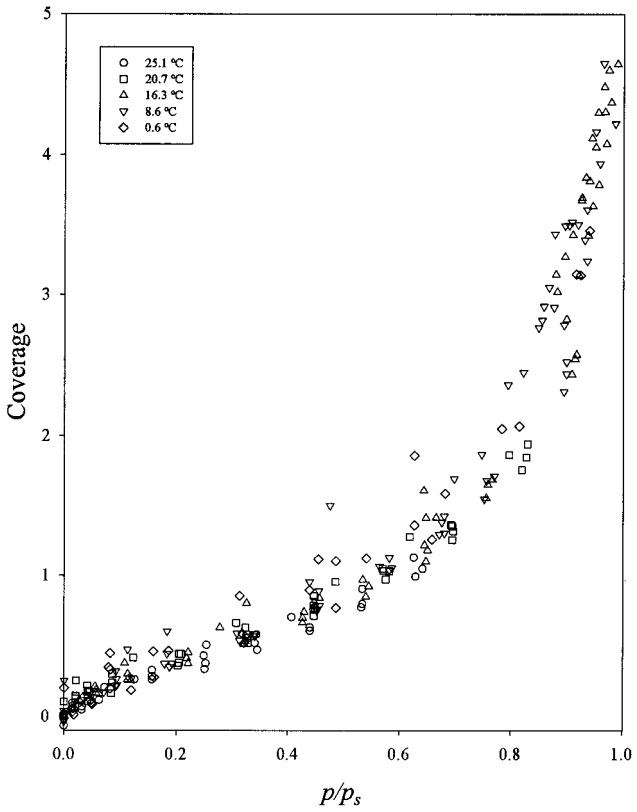

Figure 3. Absorption istherms of water onto mica for 5 temperatures. Data is shown for both ascending and descending pressures.

as a function of temperature. The coverage at a given p/p_s is greater at low temperatures, which is evident upon comparison of the 0.6 °C and 25.1 °C isotherms. These differences translate into the thermodynamic quantities we shall obtain from the isotherms in the following section.

The shape of an adsorption isotherm is indicative of the types of interactions between the substrate and adsorbing species and among the adsorbed species.[20] The shape of the isotherm also reveals how those interactions are altered with changing pressure, temperature, and coverage. The smoothness of the composite isotherm, shown in Figure 3, and the fact that it does not appear to diverge as p/p_s approaches unity are evidence that there are no phase transitions within the film at these temperatures and that water wets mica incompletely.

Layering transitions and changes in bonding networks[21] are frequently marked by abrupt changes in film thickness with pressure. The smoothness of our composite isotherm is evidence that there is no distinct layering of water adsorbed to mica and that if the bonding network of water absorbed to mica changes as a function of pressure, it does so in a continuous fashion.

Wetting is characterized by coverage (or film thickness) which diverges as coexistence between the bulk liquid and the vapor is approached. Partial wetting yields an isotherm which terminates at a finite coverage at $p/p_s = 1$. Though straightforward in theory, it is not always a simple matter to distinguish a wetting isotherm from a partially wetting one as a practical matter;[20] the isotherm may approach saturation asymptotically. In our case, the coverage increases by a factor of 2 between $p/p_s = 0.8$ and 0.95, and it does not appear to diverge but rather terminates near $\theta = 5$. Our results are consistent with the work of Beaglehole et al.,[14] who show limiting film thicknesses between 0.75 and 2.5 nm. If we assume that one layer of water has a thickness of approximately 0.25 nm,[22] then our film thickness at saturation would be 1.25 nm.

3.2 Thermodynamic Quantities. Thermodynamic analysis of the isotherms yields enthalpy and entropy as a function of coverage. From these values, the changes in intermolecular bonding among the water molecules (the hydrogen bonding network) and bonding of water to the substrate can be assessed. In addition, it will be possible to gauge the ordering of water molecules by the mica as a function of film thickness.

The equilibrium vapor pressure over the mica for a given water coverage can be written as[23]

$$\ln p_\theta = \frac{\Delta H_\theta}{RT} - \frac{\Delta S_\theta}{R} \tag{5}$$

where the subscript, θ, is a specification of the number of layers of water adsorbed to the mica. The pressure p_θ is understood to mean the relative pressure, $p_\theta/p^\ominus$, where $p^\ominus$ is a reference pressure chosen to ensure that p_θ is dimensionless. H, S, R, and T have their usual thermodynamic meaning. We determine the change in enthalpy upon adsorption for a specific coverage from the slope of a plot of $1/T$ vs $\ln(p_\theta)$. Discussion of the entropy of the system is facilitated if eq 5 is combined with its expression for bulk water ($\theta = \infty$), which gives

$$\ln\left(\frac{p_\infty}{p_\theta}\right) = \frac{\Delta H_\infty - \Delta H_\theta}{RT} - \frac{\Delta S_\infty - \Delta S_\theta}{R} \tag{6}$$

where $\Delta H_\infty = -44$ kJ mol^{-1}.[24] In this formulation, ΔH_θ is the enthalpy change when water vapor condenses into the film. Analogously, the entropy difference becomes $\Delta S_\theta \equiv S_\theta - S_g$, where S_θ is the absolute entropy of the adlayer and S_g is the absolute entropy of the vapor. Because $S_\infty = S_l$, the entropy of the bulk liquid, the entropy term in eq 6 becomes $\Delta S_\infty - \Delta S_\theta = S_l - S_\theta$, where $S_l = 69.9$ J mol^{-1} K^{-1} at 298.15 K.[25] From these quantities, the absolute entropy of the adlayers for each coverage can be calculated.

Figure 4 shows the enthalpy of adsorption and absolute entropy of the adsorbed water as a function of coverage. The dashed line in both panels of the figure delineates the values for bulk water. The error bars in coverage are derived from the uncertainty in absorbance as discussed above. The uncertainty in the cross section has not been included in the error bars in the figure since we have no way to quantify it. This uncertainty, which would be more pronounced at the lower coverages, would have the effect of shifting the coverages to lower values because the cross section should be higher for molecules bonded to the surface. The error bars in enthalpy and entropy arise principally from uncertainties in the pressure as a function of the coverage.

The condensation of water onto mica is exothermic at all coverages with an extremum at approximately $\theta = 1$. In the model that describes intermolecular bonding of water in the condensed phase,[26] each molecule, in a tetrahedral arrangement, can donate two hydrogen atoms to hydrogen bond with a neighbor and can accept two hydrogen bonds to its oxygen atom lone pairs. At submonolayer coverages, most molecules bonded to the surface are not fully tetrahedrally coordinated. We visualize this situation as islands of water molecules scattered across the mica. Water molecules on the periphery of these islands will lack neighbors with which to form intermolecular bonds, i.e., they will have dangling bonds. As more water adsorbs, near $\theta = 1$, the clusters begin to coalesce resulting in an increase in the enthalpy of condensation because water molecules can bond not only to the surface of the mica, but to neighbors laterally as well.

The entropy of adsorption mirrors the change in enthalpy. At the very lowest coverages, the water molecules are even less

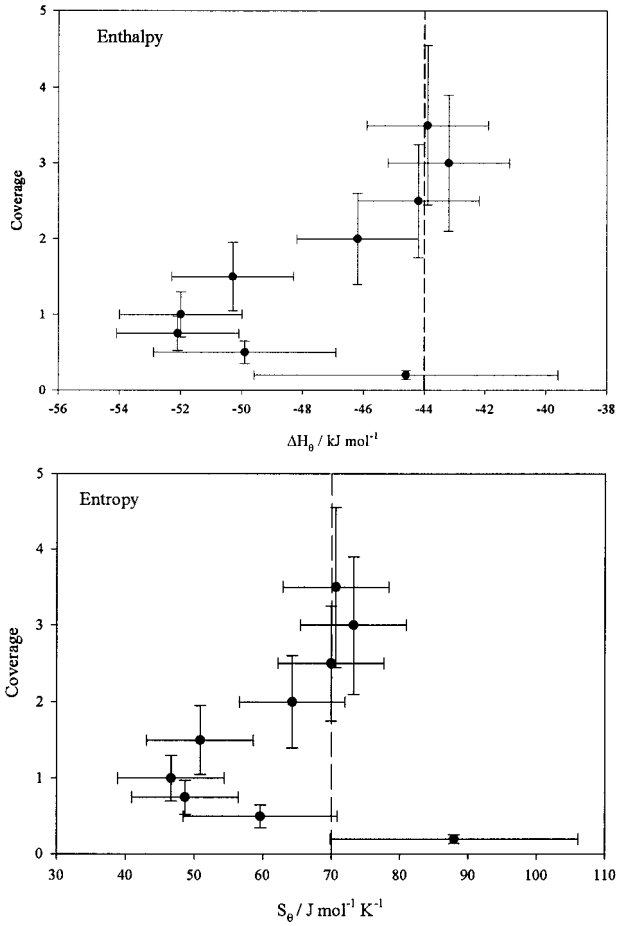

Figure 4. Enthalpy and entropy of absorption of water onto mica as a function of coverage. The dashed line in the upper panel marks the value of the enthalpy of condensation of liquid water from the vapor at 25 °C. The dashed line in the lower panel marks the absolute entropy of liquid water at 25 °C.

ordered than those in bulk water. This is demonstrated in the lower panel of Figure 4 where the entropy of the thin film near $\theta = 0.2$ actually exceeds that of the liquid. This may be a consequence of configurational entropy[27] because the islands containing small numbers of water molecules are randomly dispersed across the surface of the mica. As more water molecules are added to the surface, they are "locked" into position by their neighbors. The entropy decreases to a minimum near $\theta = 1$ implying the most ordered adlayer arrangement.

We believe that the extrema in the enthalpy and entropy at $\theta = 1$ are a consequence of the thin film structure on mica described by Miranda et al.[12] as an ice-like layer. This structure was observed to originate as polygonal islands, which had an epitaxial relationship with the substrate. As the vapor pressure was increased, the islands merged into a single layer. Subsequent layers had liquidlike characteristics. Measurements of the conductivity of water adsorbed to mica have also suggested the presence of a structured first layer.[28] Significantly, the decrease in entropy between bulk water and the entropy for $\theta = 1$ in Figure 4 is 23 ± 7 J mol^{-1} K^{-1}. The change in entropy for the liquid to crystalline phase transition for bulk water at 0 °C is 22 J mol^{-1} K^{-1}.[29] The absolute entropy of the adsorbed monolayer is therefore comparable to that of bulk ice.

As the coverage increases, $\theta > 2$, the enthalpy and entropy approach those of bulk water, indicating that the thickness of the film is increasing beyond the range of the interlayer forces.[4] As the influence of the mica is reduced, the water molecules behave more like molecules in the bulk.

3.4 Absorption Spectra. The OH stretching vibrations (ν_1,ν_3) of water are a sensitive probe of its molecular environment. This is reflected in the positions of the bands, the oscillator strengths (integrated cross sections) and the band shapes.

There is a well documented red shift in the absorption feature associated with the OH stretching vibration upon formation of hydrogen bonds.[18] This is evident upon a comparison of the water monomer with the bulk phases. The monomer has band centers at 3657 cm^{-1} (ν_1) and 3756 cm^{-1} (ν_3)[19] which collapse to a diffuse absorption centered at 3390 cm^{-1} in the liquid[19] and dropping to 3220 cm^{-1} for ice.[19] This red shift extends even further for water clusters where density functional calculations show vibrations of hydrogen bonded modes as low as the 3000 cm^{-1} region for the hexamer and octamer.[30]

The oscillator strength tends to increase with the hydrogen bond energy. For example, the integrated cross section increases by an order of magnitude for the stretching modes in going from the monomer to the liquid[18] and another factor of 1.5 on formation of ice.[31,32] The same pattern is found in the clusters with lowest oscillator strengths for the trimer with bent (strained) hydrogen bonds and highest oscillator strengths in the cyclic, nonplanar hexamer with linear hydrogen bonds.[30]

The band shape can be an indication of the heterogeneity of the molecular environment of hydrogen bonded water. In general, the more disordered the molecular environment the broader the band.[33,34] In addition to the broadening induced by the disorder, the overall width is also a consequence of the coupling of the OH vibrations of all the molecules that make up the bulk sample.[19] For clusters, the overall bandwidth is a measure of the spread of vibrational frequencies within the cluster. In the cyclic hexamer, the two stretching vibrations in each of the six isolated monomers become 12 normal modes in the complex. These range from the low oscillator strength non-hydrogen bonded (dangling bond) vibration at 3726 cm^{-1} to 3058 cm^{-1} for a vibration for a hydrogen bonded mode.[30] Experimental measurement of the cyclic water hexamer finds overlapping features that extend from 3700 to 3075 cm^{-1}.[35]

Equipped with this general review of the spectroscopic signatures of the OH stretching modes of water, we now consider thin film water on mica data.

Absorption spectra for water adsorbed to mica at high (θ = 2.5), monolayer (θ = 1), and low (θ = 0.3) coverages are shown in the three panels of Figure 5. Each measured spectrum is shown with a simulated spectrum at the corresponding coverage of bulk water. The simulation was achieved using a program written in FORTRAN for eq 1 with σ obtained from the extinction coefficient as a function of wavenumber as listed in Downing et al.[31] The value of ρt taken in eq 1 was obtained using $S_{H_2O} = \rho t$ and eq 4 at the appropriate value of θ. The mismatches between the measured and simulated spectra are due to the differences in the hydrogen bonding networks within the thin film on mica and the bulk liquid. Clearly, the measured high coverage spectrum is most like bulk liquid water and the low coverage spectrum suggests its own unique hydrogen bonded network. Although we have chosen thin films at 8.6 °C for discussion, other temperatures explored reveal the same characteristic spectroscopic profiles.

We begin exploring the adsorbed layer network for the low coverage spectra. Although we have chosen θ = 0.3 to examine in detail, other submonolayer coverage spectra down to θ = 0.1 are qualitatively similar. The most striking difference between the low coverage spectrum and the bulk water signature is its asymmetry peaking near 3350 cm^{-1} and tailing off toward 2700 cm^{-1}. The region of maximum absorption near 3350 cm^{-1}

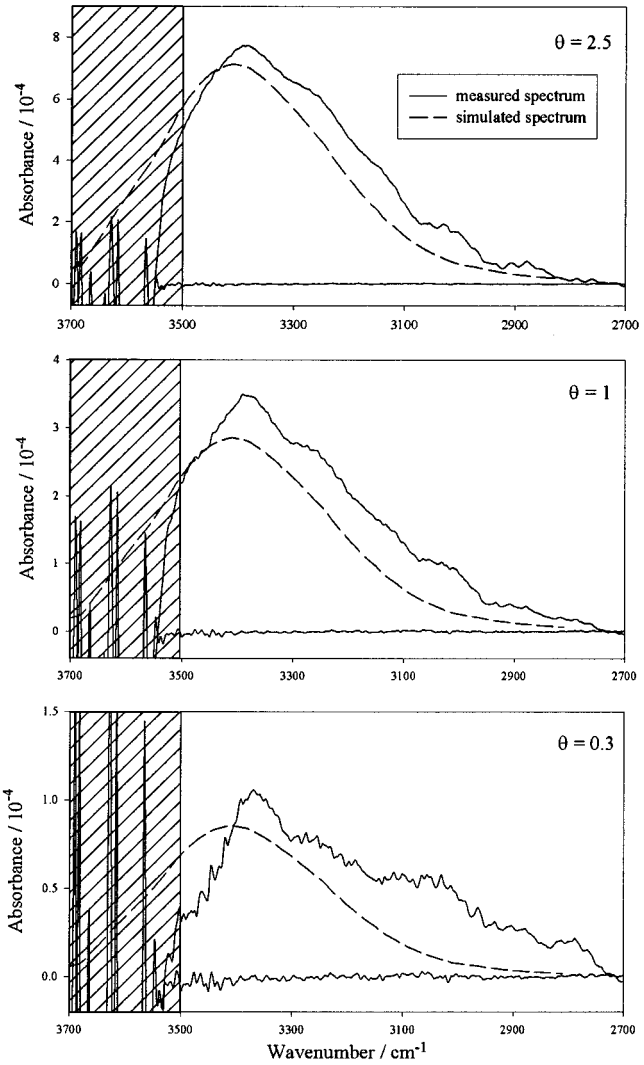

Figure 5. Absorption spectra for water adsorbed to mica for three coverages at 8.6 °C. The solid lines represent the measured spectra. The dashed lines simulate the spectra at the corresponding coverages using the optical constants of neat liquid water. Photometry in the cross hatched region is compromised because of mica's strong absorption in the region 3500 to 3700 cm^{-1}.

suggests a unique feature that might be assigned to a particular vibrational mode (perhaps the vibration of hydrogen atoms bonded to the mica). The undulations to lower wavenumbers are difficult to associate with distinct bands. However, the absorbance profile is consistent with perhaps three to five overlapping features. The absorptions between 3300 and 3000 cm^{-1} are in accord with calculated positions of vibrational modes of hexamer and higher order clusters.[30] Moreover, the molecular dynamics calculations of Odelius et al.[13] indicate the structure of the monolayer is puckered hexagons of water locked to an underlying mica substrate. These hexagons are elongated rather than regular as in I_h ice. Thus, the structured spectroscopic signature of submonolayer water on mica spanning the region around 3200 cm^{-1} is consistent with both cluster and molecular dynamics calculations. We can have a rigid submonolayer structures strongly bonded to the substrate with well developed lateral hydrogen bonds in a hexagonal network.

Our spectrum at a monolayer (θ = 1) looks more like liquid water than an ice-like bilayer, seemingly at odds with Odelius et al.'s[13] prediction. We note that the growth of adlayers on the mica surface is not a linear process. Water molecules do not occupy every adsorption site on the mica before the growth of

subsequent "layers" begins. In a Monte Carlo simulation of water on NaCl at 0.5 layers, Engkvist and Stone[36] found that the density of water molecules extended for some distance above the first layer. The molecules congregated in clusters, but the clusters were not strictly two-dimensional. The liquidlike character of the spectrum of water adsorbed to mica for $\theta = 1$ is a consequence of the fact that the coverage is for a *statistical* monolayer. Though there is one water molecule for every adsorption site, not every adsorption site is occupied. Some of the molecules will be in upper layers and adsorbed only to other water molecules, leading to the liquidlike character of the film. These considerations lead us to suggest that at the coverage of $\theta = 0.3$ and below, with few molecules in the upper layers, the islands formed may well approach the structure suggested by Odelius et al.[13]

The thicker film corresponding to $\theta = 2.5$ coverage whose optical profile is given in the upper panel of Figure 5 gives an understandable spectroscopic signature. Molecules in the upper layers are principally hydrogen bonded to neighboring water molecules. The band center of the composite spectrum is within 10 cm^{-1} of the liquid water spectrum. Poorly defined shoulders in the low wavenumber tail of the $\theta = 2.5$ adlayer spectrum resemble those that we found at 0.3, suggesting that the layer of water next to mica has retained its well ordered structure.

3.5 Mica as an Ice Nucleating Agent. We conclude by returning to the conjecture that mica could act as an effective ice nucleating agent because it has pseudohexagonal symmetry on the (001) plane and lattice constants close to those of ice.[7] The hexagonal symmetry would facilitate cooperative hydrogen bonding. This cooperative hydrogen bonding network could, in turn, expedite the liquid-crystal phase transition provided the added energy needed to overcome the strain energy added by the mismatch in lattice constants (the lattices do not match perfectly) is not prohibitive.

Mica does promote a more ordered structure in the molecules adsorbed to its surface. The infrared spectra are shifted to lower frequencies relative to the bulk water spectra, and the thermodynamic quantities show that the molecules are firmly bound to the surface and have a lower absolute entropy. However, the structure cannot be called ice. The first layer of water molecules are tightly bound to the surface, whereas subsequent layers have a more liquidlike character. This could be an indication that mica's efficacy as a heterogeneous ice nucleating agent arises not from the direct influence of the surface of the mica, but from its influence as mediated by one or more layers of water. In other words, the water molecules in direct contact with the mica may be so tightly bound that they cannot rearrange to form the ice lattice. However, molecules in adjoining layers, which are in a structured environment because of the influence of the molecules "below" them, will be able to reorganize to accommodate the crystalline structure of ice because they are not as tightly bound.

4. Conclusions

Using FTIR spectroscopy, we have found that water adsorbed to the (001) surface of muscovite mica exhibits an infrared spectrum consistent with a bonding network more structured and rigid than that of bulk water. The change in enthalpy upon adsorption indicates a strongly bonded first layer. Subsequent layers are less strongly bound with values trending toward the value for the latent heat of condensation on bulk water. The difference in entropy between bulk water and the adsorbed layer is highest for submonolayer coverages, and reveals the more ordered arrangement of water molecules. As the thickness of the film increases, the entropy difference between bulk water and the film tends to zero. The spectra suggest that mica's ability to act as an ice nucleating agent may lie in its influence as mediated by one or more layers of molecules—i.e., the critical ice embryo may not form adjacent to the mica surface, but at a distance of one or more layers away from it.

Acknowledgment. We wish to thank the National Science Foundation for support under NSF Grant No. ATM-9631838 and CHE-9816299. Charles McCrory assisted with the spectroscopic measurements. Discussions with William Schaich, Vlad Sadtchenko, and Zhenfeng Zhang are gratefully acknowledged.

References and Notes

(1) *Webster's New World Dictionary*; Warner Books: 1987.
(2) Gibbs, J. W. *Collected Works*; Longmans, Green: New York, 1928.
(3) Drude, P. *The Theory of Optics*; Longmans, Green: London, 1902.
(4) Israelachvili, J. N. *Intermolecular and Surface Forces*; Academic Press: London, 1985.
(5) Pruppacher and Klett. *Microphysics of Clouds and Precipitation*; Kluwer: Dordrecht, 1997.
(6) Langmuir, I. *J. Am. Chem. Soc.* **1918**, *40*, 1361.
(7) Turnbull, D.; Vonnegut, B. *Ind. Engng. Chem.* **1952**, *44*, 1292.
(8) Jaffray, J.; Montmory, R. *C. R. Acad. Sci.* (*Paris*) **1956**, *243*, 126. Jaffray, J.; Montmory, R. *C. R. Acad. Sci.* (*Paris*) **1956**, *243*, 891. Jaffray, J.; Montmory, R. *C. R. Acad. Sci.* (*Paris*) **1957**, *244*, 859. Jaffray, J.; Montmory, R. *C. R. Acad. Sci.* (*Paris*) **1957**, *245*, 2221.
(9) Bryant, G.; Hallett, J.; Mason, B. *J. Phys. Chem. Solids.* **1959**, *12*, 189.
(10) Elbaum, M.; Lipson, S. *Phys. Rev. Lett.* **1994**, *72*, 3562.
(11) Hu, J.; Xiao, X.-d.; Ogletree, D.; Salmeron, M. *Science* **1995**, *268*, 267.
(12) Miranda, P.; Xu, L.; Shen, Y.; Salmeron, M.; *Phys. Rev. Lett.* **1998**, *81*, 5876.
(13) Odelius, M.; Bernasconi, M.; Parrinello, M. *Phys. Rev. Lett.* **1997**, *78*, 2855.
(14) Beaglehole, D.; Christenson, H. K. *J. Phys. Chem.* **1992**, *96*, 3395. Beaglehole, D.; Radlinska, E.; Ninham, B.; Christenson, H. K.; *Phys. Rev. Lett.* **1991**, *66*, 2084.
(15) Richardson, H.; Chang, H.-C.; Noda, C.; Ewing, G. *Surf. Sci.* **1989**, *216*, 93.
(16) Born, M.; Wolf, E. *Principles of Optics*, 6th ed.; Cambridge: New York, 1998.
(17) Norton, F. H. *Elements of Ceramics*; Addison-Wesley: Cambridge, 1952.
(18) Pimentel, G.; McClellan, A. *The Hydrogen Bond*; Reinhold: New York, 1960.
(19) Eisenberg, D.; Kauzmann, W. *The Structure and Properties of Water*; Oxford, New York, 1969.
(20) Dash, J. *Phys. Rev. B.* **1977**, *15*, 3136.
(21) Foster, M.; Ewing, G. *J. Chem. Phys.* **2000**, *112*, 6817.
(22) Hobbs, P. *Ice Physics*; Clarendon: Oxford, 1974.
(23) Larher, Y. *J. Colloid Interface Sci.* **1971**, *37*, 836. Larher, Y. *J. Chim. Phys. Physicochim. Biol.* **1968**, *65*, 974.
(24) *National Research Council* (*US*) *International Critical Tables*; McGraw-Hill: New York, 1926.
(25) Weast, R., Ed.; *CRC Handbook of Chemistry and Physics*, 58th ed.; Chemical Rubber Company: Cleveland, 1977−78.
(26) Bernal, J.; Fowler, R. *J. Chem Phys.* **1933**, *1*, 515.
(27) Hill, T. L. *Introduction to Statistical Thermodynamics*; Addison-Wesley: Reading, 1960.
(28) Beaglehole, D. *Physica, A.* **1997**, *244*, 40.
(29) Atkins, P. *Physical Chemistry*, 6th ed; WH Freeman: NewYork, 1998.
(30) Estrin, E.; Paglieri, L.; Corongiu, G.; Clementi, E. *J. Phys. Chem.* **1996**, *100*, 8701.
(31) Downing, H.; Williams, D. *J. Geophys. Res.* **1975**, *80*, 1656.
(32) Irvine, W.; Pollack, J. *Icarus*. **1968**, *8*, 324.
(33) Madden, W.; Bergren, M.; McGraw, R.; Rice, S.; Sceats, M. *J. Chem. Phys.* **1978**, *69*, 3497.
(34) Wojcik, M.; Buch, V.; Devlin, J. *J. Chem. Phys.* **1993**, *99*, 2332.
(35) Pribble, R. N.; Zwier, T. S. *Science* **1994**, *265*, 75.
(36) Engkvist, O.; Stone, A. *J. Chem. Phys.* **2000**, *112*, 6827.